Observation of a Degenerate Fermi Gas Trapped by a Bose-Einstein Condensate

B. J. DeSalvo, Krutik Patel, Jacob Johansen, and Cheng Chin

James Franck Institute, Enrico Fermi Institute, and Department of Physics,
The University of Chicago, Chicago, Illinois 60637, USA

We report on the formation of a stable quantum degenerate mixture of fermionic ^{6}Li and bosonic ^{133}Cs in an optical trap by sympathetic cooling near an interspecies Feshbach resonance. New regimes of quantum degenerate Bose-Fermi mixtures are identified. With moderate attractive interspecies interactions, we show that a degenerate Fermi gas of Li can be fully confined in a Cs Bose-Einstein condensate without external potentials. For stronger attraction where mean-field collapse is expected, no such instability is observed. Potential mechanisms to explain this phenomenon are discussed.

Mixtures of atomic quantum gases are an exciting platform to study a rich variety of physics, such as the observation of heteronuclear molecules [1–7], Bose and Fermi polarons [8–13], and superfluid mixtures [14–16]. Novel quantum phases have been suggested theoretically [17–20] and probed experimentally [21–24]. Intriguing quantum excitations [25–28], mediated long-range interactions [29,30], and pairing behavior [31–33] are proposed based on degenerate Bose-Fermi mixtures.

An extensive review of previous work and specific mixtures used is found in Ref. [34]. To date, many experiments exploring quantum degenerate Bose-Fermi mixtures exhibit small to moderate mass imbalance [19,20,35–37]. For larger mass imbalance, new phenomena are expected to arise [16,33,38,39]. Light fermionic ^{6}Li and heavy bosonic ^{133}Cs yields the largest mass imbalance among stable alkali atoms. This combination offers rich interaction properties that are well characterized [40–44], and there exist interspecies Feshbach resonances at magnetic fields where both the Cs Bose-Einstein condensate (BEC) and Li Fermi gas are stable. This makes Li-Cs an excellent platform to investigate many-body physics of Bose-Fermi mixtures.

Here, we explore two novel regimes of dual-degenerate Bose-Fermi mixtures accessed by this combination of atomic species by using the tunable interactions afforded by an interspecies Feshbach resonance. First, we find that for small attractive interactions, degenerate fermions are found fully trapped and confined by the Cs BEC. Second, at large attractive scattering lengths, we find the mixture is stable in the mean-field collapse regime [18].

Our experimental procedure to prepare a quantum degenerate Bose-Fermi mixture follows. After initial laser cooling and optical trapping as described in Ref. [45], we obtain samples of 2×10^6 Li atoms in a deep translatable optical dipole trap, and 2×10^6 Cs atoms in a separate optical trap. At this point, we have a nearly equal spin mixture of Li atoms in the $F = 1/2$ hyperfine manifold, referred to here as Li$_a$ and Li$_b$, and Cs atoms spin-polarized into the $|F, m_F\rangle = |3, 3\rangle$ state, where F is the total angular momentum quantum number and m_F is the magnetic quantum number. We then ramp the magnetic field to 894.3 G. This corresponds to a scattering length for Cs of $a_{BB} = 290\ a_0$ and $a_{Li_a-Li_b} = -8330\ a_0$ for Li, where a_0 is the Bohr radius. This yields efficient evaporative cooling for Cs and the spin mixture of Li. Both species are evaporatively cooled over 10 s to approximately 300 nK. We then remove Li$_b$ with a resonant light pulse leaving only the absolute ground state of Li and Cs in the optical dipole trap.

These two species exhibit an interspecies Feshbach resonance at 892.64 G [40,42,44] that tunes the interaction between Li and Cs. Across the width of this resonance, the Cs-Cs scattering length varies slowly from $a_{BB} = 220$–280 a_0. In this range, good evaporative cooling efficiency for Cs promises the ability to sympathetically cool Li$_a$ atoms for a suitable Li-Cs scattering length. To begin sympathetic cooling, we ramp the magnetic field to 891 G ($a_{BF} = 20\ a_0$) and sequentially load both species into a dual-color optical dipole trap comprised of 785 and 1064 nm light [45]. This trap allows the cancellation of the relative gravitational sag for Li and Cs and ensures good overlap between the species at low temperatures [45]. To prepare a mixture with attractive or repulsive interspecies interactions, once the samples are mixed we ramp the magnetic field over 10 ms to either 891.9 or 893.8 G, yielding an interspecies scattering length $a_{BF} = 120$ or $-180\ a_0$, respectively. We then perform evaporative cooling for 1.5 s to obtain degenerate samples.

Detection of quantum degeneracy is performed by analyzing time-of-flight (TOF) absorption images of both species. For Cs, after evaporation we obtain a BEC of 10^4 atoms with low thermal fraction at a temperature $T_{Cs} = 20$ nK, as shown in Fig. 1(a), left panel. For thermometry of Li, we first adiabatically ramp the interspecies scattering length over 25 ms to a small value ($|a_{BF}| < 30\ a_0$) so the Cs BEC does not influence the Li cloud. We then release the atoms and image the Li after 1.5 ms expansion, as shown in the right panel of Fig. 1(a). We determine the Fermi temperature $T_F = 480(50)$ nK from the known trapping frequencies of $\omega_F = 2\pi \times (36, 430, 430)$ Hz, and
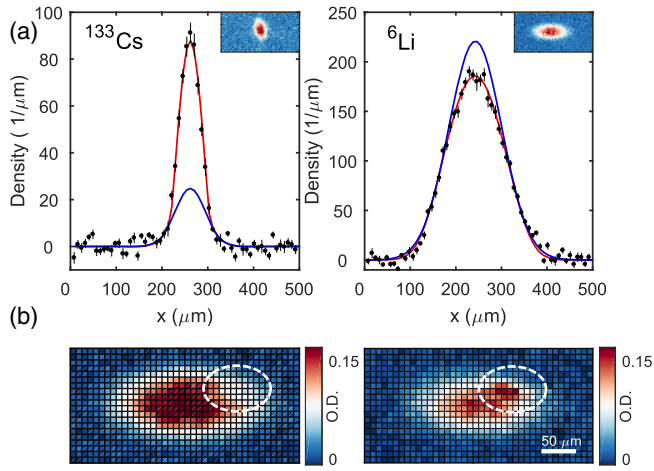
FIG. 1.   Simultaneous quantum degeneracy of ^{6}Li and ^{133}Cs.
(a) Left panel: A bimodal distribution of a Cs BEC is visible after a
30 ms TOF expansion. The blue curve indicates the thermal fraction
while the red curve shows a fit to the thermal and condensate
fraction. Right panel: For Li, a Gaussian fit to the high momentum
tail of the atoms after a 1.5 ms TOF overestimates the density at the
center (blue curve). The full distribution is fit well using a
polylogarithm function (red curve) with $T/T_F = 0.2(1)$ [46].
For repulsive interactions with $a_{BF} = 1000a_0$ [left panel (b)],
the Li density is suppressed at the location of the Cs BEC after a
1.5 ms TOF. Conversely, the Li density in the same location is
enhanced for attractive interactions with $a_{BF} = -580$ a_0 [right
panel (b)].

$T/T_F = 0.2(1)$ from fitting the absorption images using a
polylogarithm function [46]. From these fits, we observe that
sympathetic cooling works well for attractive and repulsive
interspecies interactions and both species reach deep quan-
tum degeneracy on either side of resonance.

In the presence of strong Li-Cs interaction, the density
distribution of Li is distorted. Example images are shown in
Fig. 1(b). Here, we shift the position of the Cs BEC to the edge
of the Li cloud to gain visual clarity of the effect. For repulsive
interactions [Fig. 1(b), left panel], Li is repelled from the
BEC. Conversely, for attractive interactions [Fig. 1(b) right
panel], Li atoms are attracted to the Cs BEC.

Per mean field theory, the potential experienced by one
atomic species due to interspecies interactions is given by
$2\pi\hbar^2 a_{BF}(1/m_B + 1/m_F)n(\vec{r})$, where $m_{F(B)}$ is the mass of
the fermion (boson), $\hbar$ is the reduced Planck's constant, and
$n(\vec{r})$ is the density distribution of the other species. In our
case, the density of the Cs BEC is over one order of
magnitude larger than the Li degenerate Fermi gas, so the
potential experienced by the Li is significantly greater.
Given the typical density of a Cs BEC of $n_B =
5 \times 10^{13}$ cm^{-3}, for $a_{BF} = -500$ a_0 the trap depth in
temperature units felt by Li is 450 nK. This large depth
suggests that Li can be loaded into the Cs BEC even in the
absence of another confining potential.

To investigate this possibility experimentally, we per-
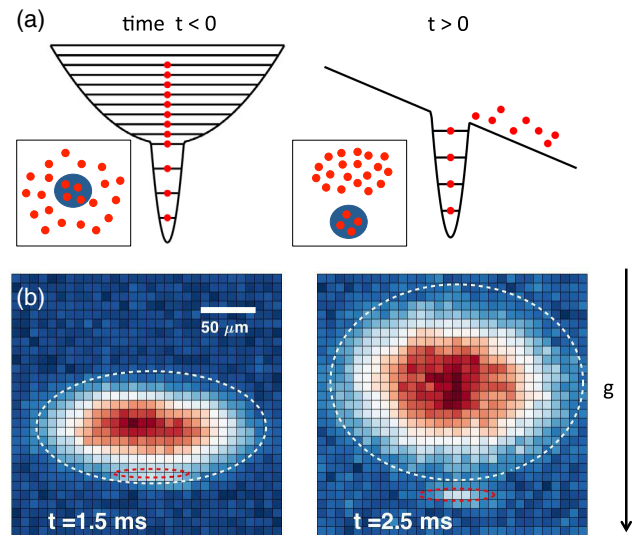form a Stern-Gerlach sequence to separate the Li atoms

FIG. 2.   Stern-Gerlach separation of Li atoms trapped in a Cs
BEC. Shown schematically in (a), strong attractive interspecies
interactions confine a fraction of Li atoms (red dots) within the Cs
BEC (blue circle). At $t = 0$ we remove the optical trap and apply
a magnetic field gradient to separate those trapped from the rest of
the sample. Example images of Li after a short TOF are shown in
(b). Dashed red circles indicate the position and size of the BEC
at the imaging time and the white dashed line indicates the Fermi
radius.

trapped by the Cs BEC from those that are not, as depicted in
Fig. 2(a). We first prepare a degenerate Bose-Fermi mixture
in a single beam trap by performing our usual sequence and
slowly ramping the intensity of the 785 nm beam to zero. In
this simplified configuration, the overlap of the two species is
controlled by the magnetic field gradient, and we obtain trap
frequencies of $\omega_B = 2\pi \times (6.5, 130, 160)$ Hz for Cs and
$\omega_F = 2\pi \times (36, 400, 400)$ Hz for Li. Next, we ramp the
magnetic field gradient to 4 G/cm providing a force against
gravity and simultaneously increase the interaction strength
to $-650a_0$ over 30 ms. This deepens the potential so a
reasonable number of Li are trapped and shifts the Li up such
that the Cs BEC sits on the lower edge of the Li cloud. We
then extinguish the optical trap while leaving the magnetic
field and gradient on. The magnetic field gradient is sufficient
to overlevitate Li, but not the Cs atoms. Therefore, Li atoms
trapped by Cs BEC fall downwards.

Results of this experiment are shown in the absorption
images of Li after a varying TOF, see Fig. 2(b). In each image,
the white dashed curve shows the maximum extent of the
cloud from the calculated Fermi radius and the red dashed
curve shows the position and spatial extent of the Cs BEC.
After a TOF, Li atoms trapped in the Cs BEC spatially
separate from the rest of the sample. These Li atoms are
contained in the volume of the Cs BEC and follow its
trajectory over the entire TOF. Once spatially separated, Li
atoms trapped in the Cs BEC can be counted. By following
the previously described Stern-Gerlach procedure at different
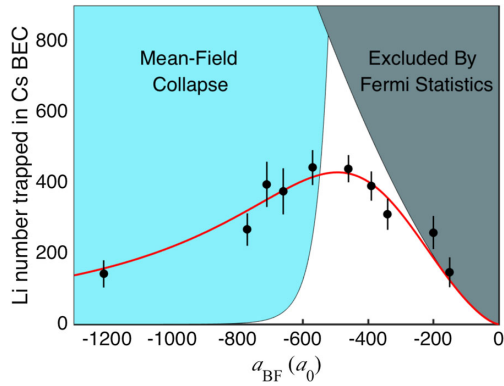magnetic field values, we measure the number of Li atoms

FIG. 3.   Number of Li atoms trapped in Cs BEC. As a function of the interspecies scattering length a_{BF} at the end of the magnetic field ramp, we measure the number of Li atoms trapped in the Cs BEC after a 1.5 ms Stern-Gerlach separation (black dots). Within the approximation described in the text, the grey shaded region represents the region excluded by Fermi statistics and the blue shaded area indicates the region where mean-field collapse is expected. The red curve shows a fit based on a rate equation model describing the steady-state number of atoms trapped by the Cs BEC (see text).

trapped by the Cs BEC as a function of a_{BF} as shown in Fig. 3.

Owing to the Pauli exclusion principle, there is a limited number of Li atoms $N < N_{max}$ that can be trapped within the Cs BEC. Assuming the density of the BEC is not perturbed by Li atoms, the maximum number N_{max} can be found analytically. Within the mean-field and Thomas-Fermi approximations, the density distribution of the BEC is an inverted parabola, yielding a harmonic trap for Li with trap depth $U_0 = \frac{1}{2}(m_B/m_F + 1)(|a_{BF}|/a_{BB})\mu$ and trapping frequency $\omega_{trap} = [\frac{1}{2}(m_B/m_F)(m_B/m_F + 1)|a_{BF}|/a_{BB}]^{1/2}\omega_B$, where ω_B is the trapping frequency for Cs and μ is its chemical potential. Notably the trap frequency for Li ω_F is 16 times larger than the trap frequency for Cs due to mass imbalance alone. Therefore, the dynamics of Li in the Cs BEC are much faster than the condensate itself.

By setting the Fermi energy equal to the trap depth, one finds that for $a_{BF} < 0$ the maximum number of Li trapped by the Cs BEC is

$$N_{max} = \frac{1}{12\sqrt{2}}\left[\left(1 + \frac{m_F}{m_B}\right)\frac{|a_{BF}|}{a_{BB}}\right]^{3/2}\left(\frac{\mu}{\hbar\omega_B}\right)^3. \quad (1)$$

This limit is indicated by the grey shaded region in Fig. 3 and is consistent with our measurement for $|a_{BF}| < 400 \, a_0$. For these weak interactions, since the number of Li trapped is close to the maximum, the Li remains deeply quantum degenerate.

For a large negative scattering length, mean-field calculations predict another limit on the number of Li atoms that can be trapped by the Cs BEC. When the Li density exceeds a critical value n_{crit}, theory predicts a collapse of the mixture

due to the loss of mechanical stability. For a homogenous gas, the critical density is [18]

$$n_{crit} = \frac{4\pi}{3}\frac{m_B^3 m_F^3}{(m_B + m_F)^6}\frac{a_{BB}^3}{a_{BF}^6}. \quad (2)$$

The condition for collapse in a trapped gas is found following the numerical procedure described in Ref. [18]. We find that the system collapses when the peak density of the fermions exceeds the critical density given in Eq. (2). This limit sets the lower boundary of the shaded blue region in Fig. 3. Shown in Fig. 3 as well as observed in other experiments including a longer hold time, for large negative scattering lengths a_{BF} we find significantly more Li atoms trapped in the Cs BEC than permitted by mean-field theory.

One possible explanation for the lack of mean-field collapse is beyond mean-field terms similar to the Lee-Huang-Yang term for bosons [47]. Observed in dipolar quantum gases [48], this effect leads to a short-range repulsion and stabilizes a collapsing BEC with dipolar interactions, and likely a Bose-Bose mixture with strong interspecies attraction [49]. The scenario to stabilize an attractive Bose-Fermi mixture with beyond mean-field effects [50] requires further theoretical investigation.

In our system, another possible explanation for the lack of mean-field collapse is a dynamical process including three-body loss and Fermi statistics. The association of higher particle number with collisional loss seems counterintuitive, but the strong density dependence of three-body collisions is key to removing atoms preferentially from the high-density region and preventing mean-field collapse.

To explore this possibility, we suggest the following model. Since the dynamical time scale for Li is much shorter than for Cs, we describe the density of Li atoms trapped in the Cs BEC as

$$\frac{dn}{dt} = Aa_{BF}^2 n_F n_B f - Ba_{BF}^4 n_B^2 n, \quad (3)$$

where A and B are constants, n_B is the density of the Cs BEC, n is the density of Li confined in the BEC, and n_F is the density of unconfined Li. The first term accounts for elastic collisions that populate available states in the BEC potential with probability $f \approx 1 - N/N_{max}$ given by Fermi statistics. The second term represents three-body loss due to Li-Cs-Cs collisions [51].

Because of the small number of Li atoms trapped in the Cs BEC and the large separation in dynamical time scales between the two species, we assume that the BEC density profile and Cs number are not disturbed in the time the Li density profile reaches steady state. Averaging Eq. (3) over the extent of the Cs BEC, we obtain $d\bar{n}/dt = A'a_{BF}^2 \bar{n}_B \bar{n}_F f - B'a_{BF}^4 \bar{n}_B^2 \bar{n}$, where $\bar{x}$ is the averaged value of x, and A' and B' are constants incorporating geometric factors from averaging.

In steady-state $d\bar{n}/dt = 0$, we obtain $N = N_{max}/(1 + Ca_{BF}^2 N_{max})$, where C is a constant. Combining this expression with Eq. (1), we fit our data in Fig. 3 with C as the only fitting parameter. The result yields good agreement. In the case of no collisional loss $B' = 0$, the fit function reproduces the limit where a deeply degenerate Fermi gas of N_{max} Li atoms is supported by the BEC.

In this picture, for large negative scattering length, Li atoms are quickly lost through recombination. Since this process is the highest at the center of the BEC, the loss of Li atoms prevents the runaway density build up at the trap center. Similar loss of Cs atoms occurs predominately at the trap center. However, the loss of Cs is slowed by the limited rate at which its volume is replenished with fermions from the surrounding Fermi gas.

In Fig. 4, we show the evolution dynamics of a Cs BEC immersed in the Li degenerate Fermi gas. Here, we first create a degenerate mixture in the single beam dipole trap. After quickly ramping the magnetic field to a desired value, we measure the number of Cs atoms in the condensate after a TOF. The atom number in the BEC smoothly decays with a loss rate proportional to a_{BF}^4 as expected [52]. No dramatic drop in atom number associated with collapse is observed.

Mean-field calculations assume that the system thermalizes quickly enough to reach equilibrium. However, thermalization is known to be slow for systems with large mass imbalance. Unlike atoms must undergo $\xi = 3(m_B + m_F)^2/(4m_B m_F)$ collisions to thermalize [53]. An estimation of the collision rate between degenerate Bose and Fermi gases is in general complicated, and we employ a model for thermal gases that offers an upper bound on the collision rate given by $\gamma = 4\pi a_{BF}^2 \bar{v} \int d^3 r\, n_F'(\vec{r}) n_B(\vec{r})$, where $n_F'(\vec{r})$ is the density of fermions available for collisions and the averaged relative velocity of Li and Cs atoms is given by $\bar{v} \approx \sqrt{2E_F/m_F}$ in our experiment. Combining the above results with the fermion density's slow variation across the BEC, we obtain the thermalization rate $\Gamma = (N_F' + N_B/N_F' N_B)(\gamma/\xi)$ [54] as

$$\Gamma \approx 3.74 \frac{m_B m_F^2}{(m_B + m_F)^2} \frac{(N_B + N_F')}{N_F'^{1/3}} \frac{a_{BF}^2 \bar{\omega}_F^2}{\hbar}, \quad (4)$$

where $\bar{\omega}_F$ is the geometric mean of the trap frequencies of the fermions, N_B is the number of bosons, and N_F' is the number of fermions participating in collisions. Using $N_F' \approx g(E_F)k_B T = 3N_F(T/T_F)$ where $g(\epsilon)$ is the single particle density of states, we obtain the thermalization rate, shown in Fig. 4(b).

At large scattering lengths $|a_{BF}| > 520a_0$, the loss rate exceeds the thermalization rate, suggesting the mixture will deviate from thermal equilibrium. Notably, the dominance of inelastic loss is more likely to occur in a Li-Cs system due to its strong mass imbalance. In comparison to the ^{40}K-^{87}Rb mixture in Refs. [19,20] where mean-field collapse was reported, our thermalization rate is 2 times lower [from Eq. (4)], while the three-body collision rate increases by a factor of 2 [52] for the same trap frequency and atom numbers. Consequently, our system with large attractive Li-Cs interactions likely reaches a dynamical equilibrium where fast loss allows the mixture to survive for much longer than the mean-field expectation.

In conclusion, we report the first quantum degenerate mixture of Li and Cs and use this system to probe novel regimes of Bose-Fermi mixtures. For weak attractive interactions, a degenerate Fermi gas with few hundred Li atoms is confined within the BEC. This represents an intriguing quantum object well suited for future study. For strong attractive interactions, we observe that the system is stable against mean-field collapse. We present one possible model to explain this observation based on the relative time scales of loss and thermalization. Other possible explanations involving beyond mean-field effects are under investigation. The lack of the mean-field collapse in our system allows us to explore a region of the Bose-Fermi mixture that was previously thought inaccessible.
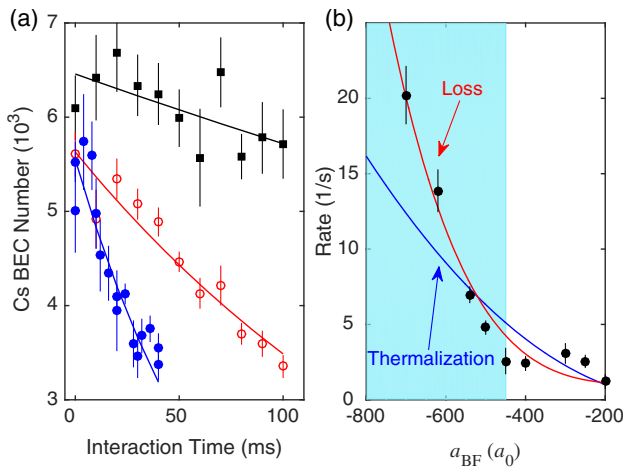

FIG. 4. Loss dynamics of Cs BEC immersed in Li degenerate Fermi gas. (a) Atom number in Cs BEC for $a_{BF} = -200$ (black), -500 (red), and $-620\, a_0$ (blue). The data are well described by smooth exponential loss (solid lines). The $1/e$ loss rates extracted from these fits shown in panel (b) are well fit by the expected a_{BF}^4 scaling including a constant offset in the loss rate to account for measured Cs-Cs-Cs recombination (red line). An estimation of the thermalization rate (see text) is indicated by the solid blue curve. The loss rate exceeds the thermalization rate at $a_{BF} = -520a_0$, above which the system no longer reaches thermal equilibrium.

[1] T. Takekoshi, L. Reichsöllner, A. Schindewolf, J. M. Hutson, C. R. Le Sueur, O. Dulieu, F. Ferlaino, R. Grimm, and H. C. Nägerl, Phys. Rev. Lett. **113**, 205301 (2014).

[2] K. K. Ni, S. Ospelkaus, M. H. G. de Miranda, A. Pe'er, B. Neyenhuis, J. J. Zirbel, S. Kotochigova, P. S. Julienne, D. S. Jin, and J. Ye, Science **322**, 231 (2008).

[3] M. S. Heo, T. T. Wang, C. A. Christensen, T. M. Rvachov, D. A. Cotta, J. H. Choi, Y. R. Lee, and W. Ketterle, Phys. Rev. A **86**, 021602(R) (2012).

[4] S. D. Kraft, P. Staanum, J. Lange, L. Vogel, R. Wester, and M. Weidemüller, J. Phys. B **39**, S993 (2006).

[5] R. Roy, R. Shrestha, A. Green, S. Gupta, M. Li, S. Kotochigova, A. Petrov, and C. H. Yuen, Phys. Rev. A **94**, 033413 (2016).

[6] J. W. Park, S. A. Will, and M. W. Zwierlein, Phys. Rev. Lett. **114**, 205302 (2015).

[7] A.-C. Voigt, M. Taglieber, L. Costa, T. Aoki, W. Wieser, T. W. Hänsch, and K. Dieckmann, Phys. Rev. Lett. **102**, 020405 (2009).

[8] M. G. Hu, M. J. Van De Graaff, D. Kedar, J. P. Corson, E. A. Cornell, and D. S. Jin, Phys. Rev. Lett. **117**, 055301 (2016).

[9] N. B. Jørgensen, L. Wacker, K. T. Skalmstang, M. M. Parish, J. Levinsen, R. S. Christensen, G. M. Bruun, and J. J. Arlt, Phys. Rev. Lett. **117**, 055302 (2016).

[10] C. Kohstall, M. Zaccanti, M. Jag, A. Trenkwalder, P. Massignan, G. M. Bruun, F. Schreck, and R. Grimm, Nature (London) **485**, 615 (2012).

[11] A. Schirotzek, C. H. Wu, A. Sommer, and M. W. Zwierlein, Phys. Rev. Lett. **102**, 230402 (2009).

[12] F. Scazza, G. Valtolina, P. Massignan, A. Recati, A. Amico, A. Burchianti, C. Fort, M. Inguscio, M. Zaccanti, and G. Roati, Phys. Rev. Lett. **118**, 083602 (2017).

[13] M. Cetina, M. Jag, R. S. Lous, J. T. M. Walraven, R. Grimm, R. S. Christensen, and G. M. Bruun, Phys. Rev. Lett. **115**, 135302 (2015).

[14] R. Roy, A. Green, R. Bowler, and S. Gupta, Phys. Rev. Lett. **118**, 055301 (2017).

[15] I. Ferrier-Barbut, M. Delehaye, S. Laurent, A. Grierm, B. Rem, F. Chevy, and C. Salomon, Science **345**, 1035 (2014).

[16] X. C. Yao, H. Z. Chen, Y. P. Wu, X. P. Liu, X. Q. Wang, X. Jiang, Y. Deng, Y. A. Chen, and J. W. Pan, Phys. Rev. Lett. **117**, 145301 (2016).

[17] F. M. Marchetti, C. J. M. Mathy, D. A. Huse, and M. M. Parish, Phys. Rev. B **78**, 134517 (2008).

[18] K. Mølmer, Phys. Rev. Lett. **80**, 1804 (1998).

[19] M. Zaccanti, C. D'Errico, F. Ferlaino, G. Roati, M. Inguscio, and G. Modugno, Phys. Rev. A **74**, 041605(R) (2006).

[20] S. Ospelkaus, C. Ospelkaus, L. Humbert, K. Sengstock, and K. Bongs, Phys. Rev. Lett. **97**, 120403 (2006).

[21] K. Sengupta, N. Dupuis, and P. Majumdar, Phys. Rev. A **75**, 063625 (2007).

[22] M. Lewenstein, L. Santos, M. A. Baranov, and H. Fehr-mann, Phys. Rev. Lett. **92**, 050401 (2004).

[23] T. Best, S. Will, U. Schneider, L. Hackermüller, D. van Oosten, I. Bloch, and D. S. Lühmann, Phys. Rev. Lett. **102**, 030408 (2009).

[24] K. Gunter, T. Stoferle, H. Moritz, M. Kohl, and T. Esslinger, Phys. Rev. Lett. **96**, 180402 (2006).

[25] J. Santhanam, V. M. Kenkre, and V. V. Konotop, Phys. Rev. A **73**, 013612 (2006).

[26] S. K. Adhikari, Phys. Rev. A **72**, 053608 (2005).

[27] T. Karpiuk, K. Brewczyk, S. Ospelkaus-Schwarzer, K. Bongs, M. Gajda, and K. Rzążewski, Phys. Rev. Lett. **93**, 100401 (2004).

[28] T. Karpiuk, M. Brewczyk, and K. Rzążewski, Phys. Rev. A **73**, 053602 (2006).

[29] M. J. Bijlsma, B. A. Heringa, and H. T. C. Stoof, Phys. Rev. A **61**, 053601 (2000).

[30] S. De and I. B. Spielman, Appl. Phys. B **114**, 527 (2014).

[31] D. V. Efremov and L. Viverit, Phys. Rev. B **65**, 134519 (2002).

[32] E. Fratini and P. Pieri, Phys. Rev. A **81**, 051605(R) (2010).

[33] S. Gopalakrishnan, C. V. Parker, and E. Demler, Phys. Rev. Lett. **114**, 045301 (2015).

[34] R. Onofrio, Phys. Usp. **59**, 1129 (2016).

[35] M. Taglieber, A.-C. Voigt, T. Aoki, T. W. Hänsch, and K. Dieckmann, Phys. Rev. Lett. **100**, 010401 (2008).

[36] J. W. Park, C.-H. Wu, I. Santiago, T. G. Tiecke, S. Will, P. Ahmadi, and M. W. Zwierlein, Phys. Rev. A **85**, 051602(R) (2012).

[37] V. D. Vaidya, J. Tiamsuphat, S. L. Rolston, and J. V. Porto, Phys. Rev. A **92**, 043604 (2015).

[38] E. Fratini and P. Pieri, Phys. Rev. A **85**, 063618 (2012).

[39] A. Banerjee, J. Phys. B **42**, 235301 (2009).

[40] S. K. Tung, C. Parker, J. Johansen, C. Chin, Y. Wang, and P. S. Julienne, Phys. Rev. A **87**, 010702(R) (2013).

[41] S. K. Tung, K. Jimenez-Garcia, J. Johansen, C. V. Parker, and C. Chin, Phys. Rev. Lett. **113**, 240402 (2014).

[42] J. Johansen, B. J. DeSalvo, K. Patel, and C. Chin, Nat. Phys. **13**, 731 (2017).

[43] J. Ulmanis, S. Häfner, R. Pires, E. D. Kuhnle, M. Weide-müller, and E. Tiemann, New J. Phys. **17**, 055009 (2015).

[44] M. Repp, R. Pires, J. Ulmanis, R. Heck, E. D. Kuhnle, M. Weidemüller, and E. Tiemann, Phys. Rev. A **87**, 010701 (2013).

[45] J. Johansen, Ph.D. thesis, University of Chicago, 2017.

[46] W. Ketterle and M. W. Zwierlein, in *Proceedings of the International School of Physics Enrico Fermi, Ultracold Fermi Gases,* Course CLXIV (IOS Press, Amsterdam, 2006).

[47] T. D. Lee, K. Huang, and C. N. Yang, Phys. Rev. **106**, 1135 (1957).

[48] I. Ferrier-Barbut, H. Kadau, M. Schmitt, M. Wenzel, and T. Pfau, Phys. Rev. Lett. **116**, 215301 (2016).

[49] D. S. Petrov, Phys. Rev. Lett. **115**, 155302 (2015).

[50] A. P. Albus, S. A. Gardiner, F. Illuminati, and M. Wilkens, Phys. Rev. A **65**, 053607 (2002).

[51] E. Braaten and H. W. Hammer, Phys. Rep. **428**, 259 (2006).

[52] J. P. D'Incao and B. D. Esry, Phys. Rev. A **73**, 030702(R) (2006).

[53] G. Delannoy, S. G. Murdoch, V. Boyer, V. Josse, P. Bouyer, and A. Aspect, Phys. Rev. A **63**, 051602(R) (2001).

[54] A. Mosk, S. Kraft, M. Mudrich, K. Singer, W. Wohlleben, R. Grimm, and M. Weidemüller, Appl. Phys. B **73**, 791 (2001).